Phenomenology of U(1) (L_mu - L_tau) charged DM at PAMELA and colliders

Based on Baek and Ko, arXiv:0811.1646
JCAP 0910.011 (2009)

Talk at DESY Workshop on
IDMS 2011, June 14-17, 2011

DM in the Universe

Although 23% of the universe is composed of DM, we do not know its nature yet!!

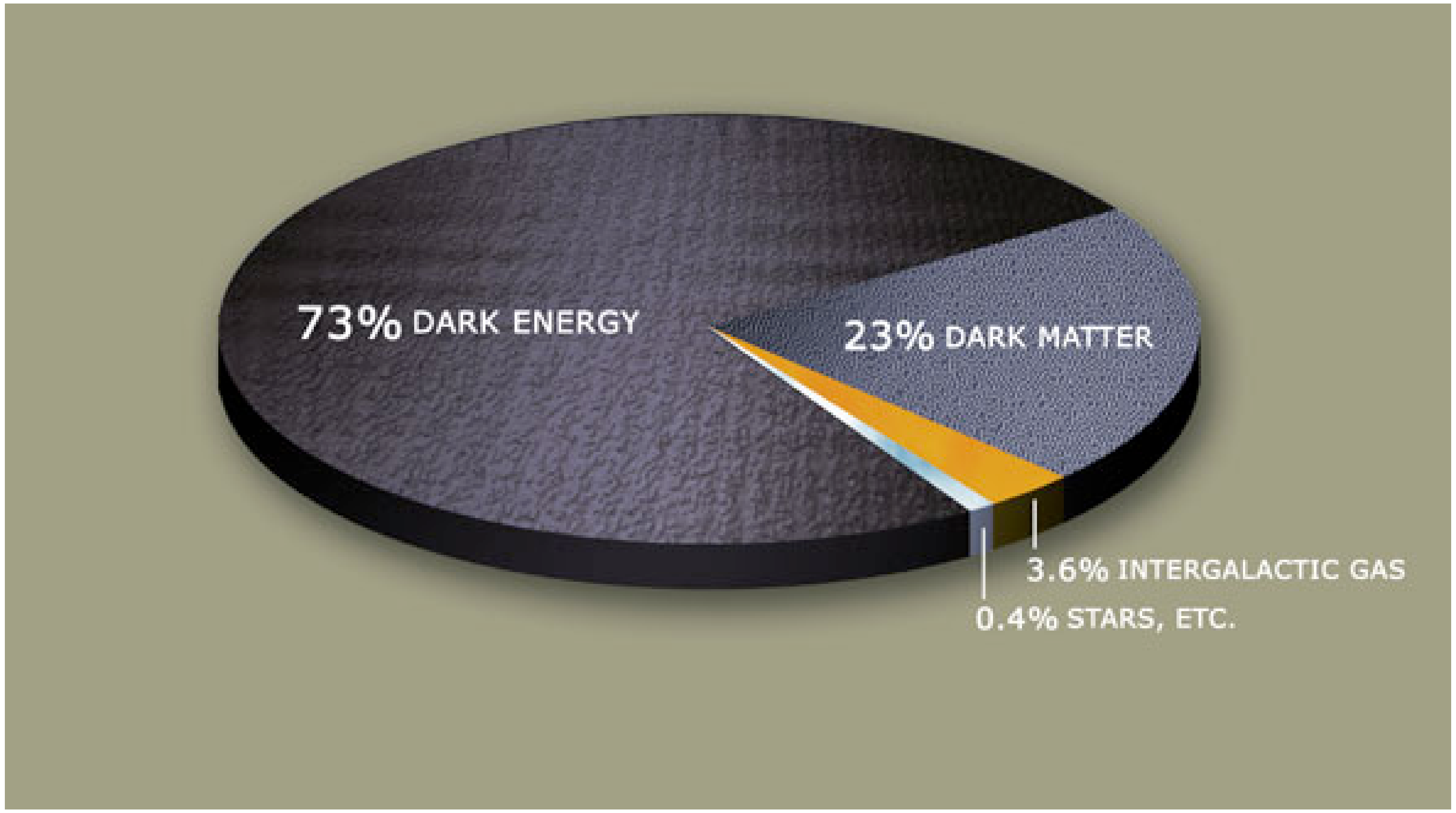

Nature of CDM('s) ?

- mass, spin, quantum numbers ?
- Direct detection
- Indirect detection
- Collider search
- All of these are complementary with each other
- For complete study, better to work on specific model lagrangian one by one

PAMELA positron excess

- PAMELA reports positron access @ high energy
- PAMELA reports no access in antiproton
- ATIC/PPB-BETS : excess in (e+ + e-) around 500-800 GeV
- Combining these observations, one can conclude
- Leptophilic DM, OR
- Very heavy DM (> 10 TeV) with dominant DM + DM -> W+ W- (and also into ZZ , HH)

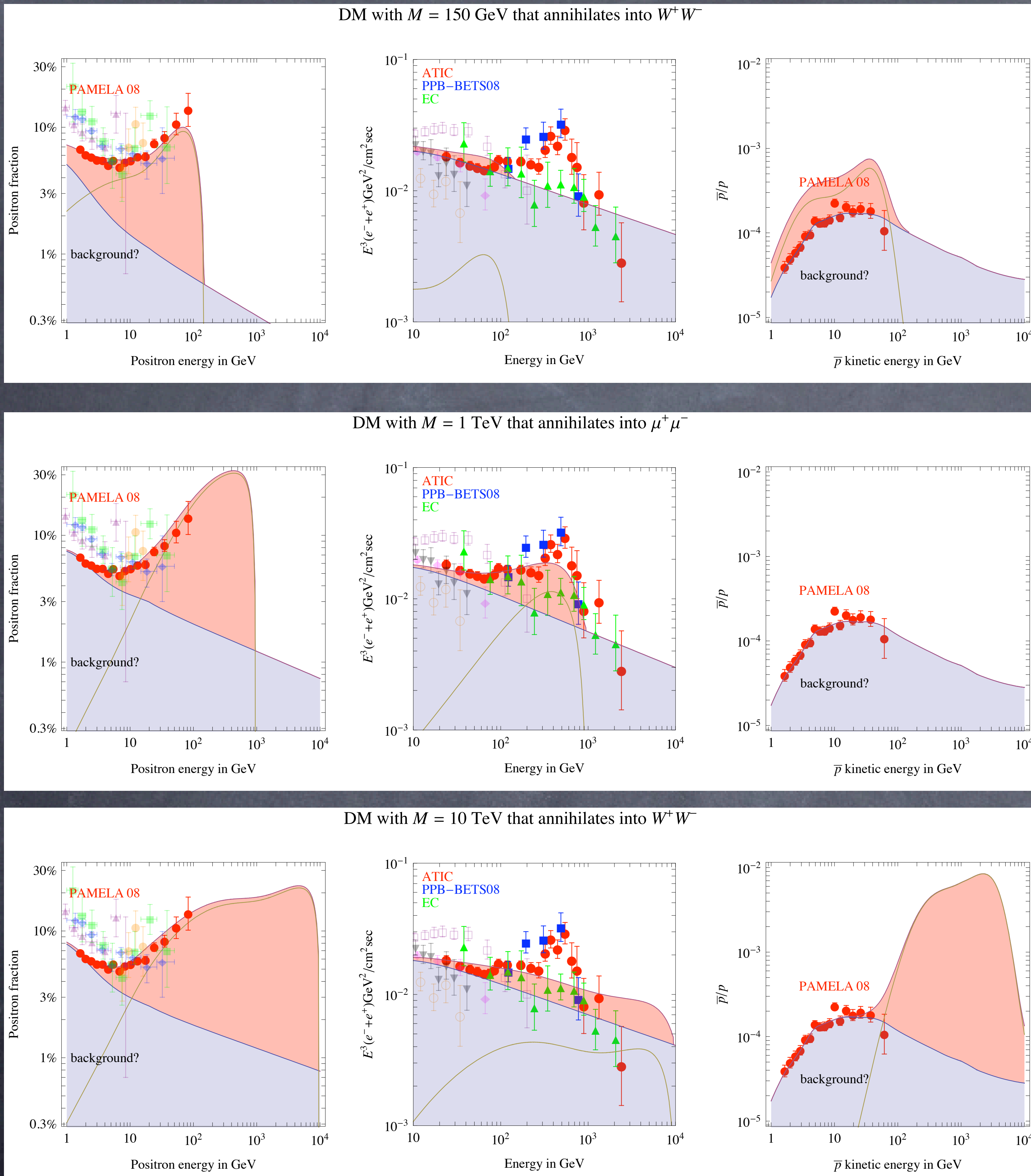

Cirelli, Strumia et al. NPB

e+, (e- + e+), pbar from left, center, and right

DM interpretation

- We need leptophilic DM decaying preferentially into $\mu^+\mu^-$ or $\tau^+\tau^-$
- π^0 from τ decays into $\gamma\gamma$. Need to consider gamma-ray constraints.
- In general there can be associated ν productions. Need to consider ν constraints.

$U(1)_{L_\mu - L\tau}$ model

- Anomaly free subgroup of SM : one of

$$B-L\ , L_e - L_\mu\ , L_\mu - L_\tau\ , L_e - L_\tau$$

- Least constrained one : $L_\mu - L_\tau$
- Foot, He, Volkas, et al. in late 80's
- This could be an example of horizontal gauge symmetries that often invoked for flavor physics
- PAMELA positron excess and collider signature (Baek and Ko, in this talk)

Qutumn number assignments

	SU(3)	SU(2)	$U(1)_Y$	$U(1)_{L_\mu - L_\tau}$
Q	3	2	1/6	0
u^c	$\overline{3}$	1	-2/3	0
d^c	$\overline{3}$	1	1/3	0
L	1	2	-1/2	(0,1,-1)
e^c	1	1	1	(0,-1,1)
H	1	2	1/2	0

- SM singlet Higgs field ϕ is introduced

	SU(3)	SU(2)	$U(1)_Y$	$U(1)_{L_\mu - L_\tau}$
ϕ	1	1	0	1

- The $U(1)'$ breaking scale is independent of the ew scale

$$m_{Z'} = g' v_\phi .$$

2011년 6월 15일 수요일

U(1)′ charged Dirac fermion DM

	SU(3)	SU(2)	$U(1)_Y$	$U(1)_{L_\mu - L_\tau}$
ϕ	1	1	0	1
ψ_D	1	1	0	1
ψ_D^c	1	1	0	-1

Thermal relic density of the CDM ψ_D

$$\psi_D \overline{\psi}_D \to Z^{'*} \to \ell^+ \ell^-, \nu_\ell \overline{\nu}_\ell, \;\; (\ell = \mu, \tau),$$

$$\psi_D \overline{\psi}_D \to Z' Z'$$

$$\mathcal{L}_{\rm Model} = \mathcal{L}_{\rm SM} + \mathcal{L}_{\rm New}$$

$$\mathcal{L}_{\rm New} = -\frac{1}{4} Z^{'}_{\mu\nu} Z^{'\mu\nu} + \overline{\psi_D} i D \cdot \gamma \psi_D - M_{\psi_D} \overline{\psi_D} \psi_D + D_\mu \phi^* D^\mu \phi$$
$$-\lambda_\phi (\phi^* \phi)^2 - \mu_\phi^2 \phi^* \phi - \lambda_{H\phi} \phi^* \phi H^\dagger H.$$

Here we ignored kinetic mixing for simplicity

$$D_\mu = \partial_\mu + ieQA_\mu + i\frac{e}{s_W c_S}(I_3 - s_W^2 Q) Z_\mu + ig^{'} Y^{'} Z^{'}_\mu$$

We will study the following observables:
Muon g-2, Leptophilc DM, Collider Signature

Muon (g-2)

$$\Delta a_\mu = a_\mu^{\rm exp} - a_\mu^{\rm SM} = (302 \pm 88) \times 10^{-11}.$$

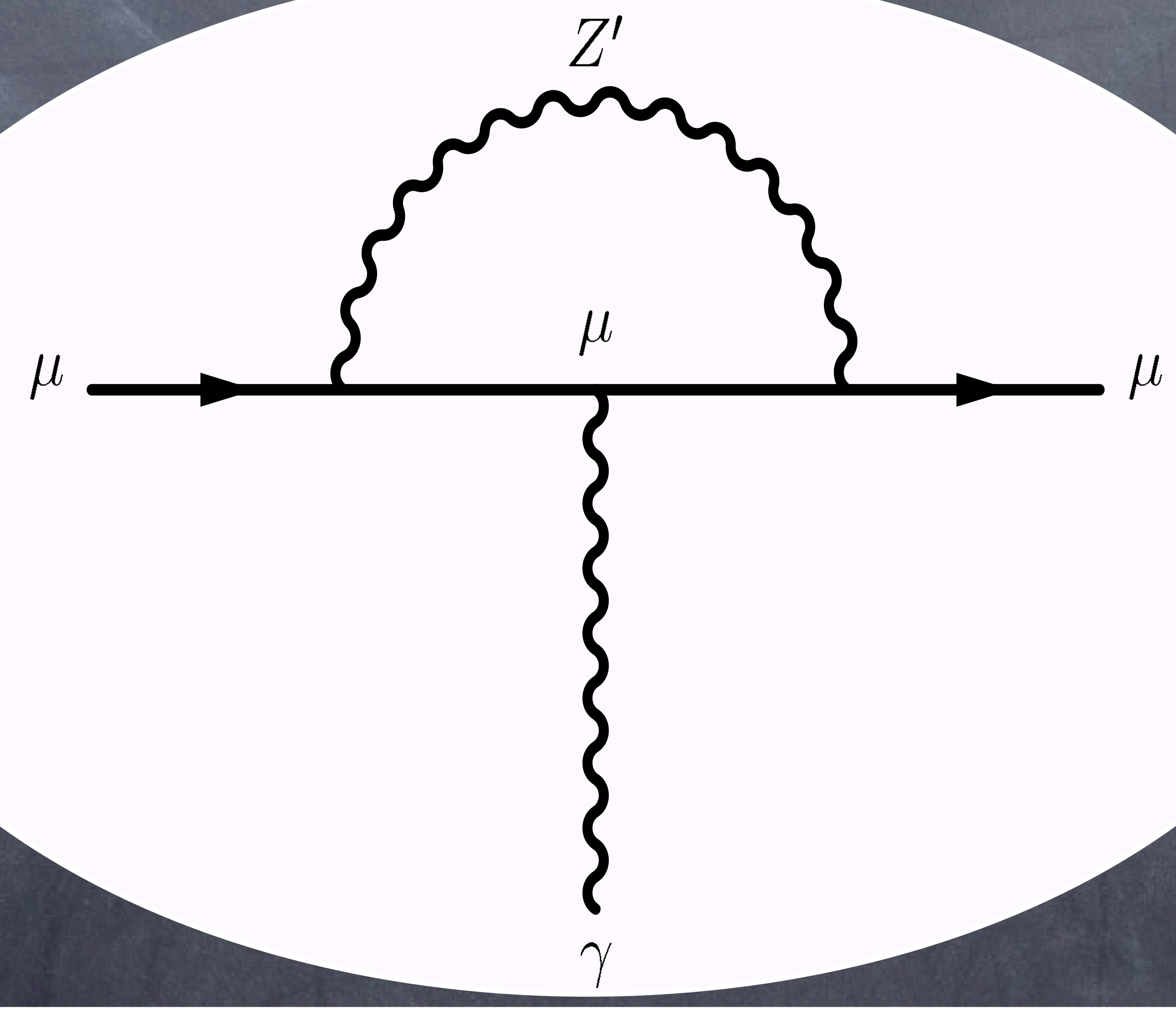

$$\Delta a_\mu = \frac{\alpha'}{2\pi} \int_0^1 dx \frac{2m_\mu^2 x^2 (1-x)}{x^2 m_\mu^2 + (1-x) M_{Z'}^2} \approx \frac{\alpha'}{2\pi} \frac{2m_\mu^2}{3M_{Z'}^2}$$

Prediction for muon (g-2)

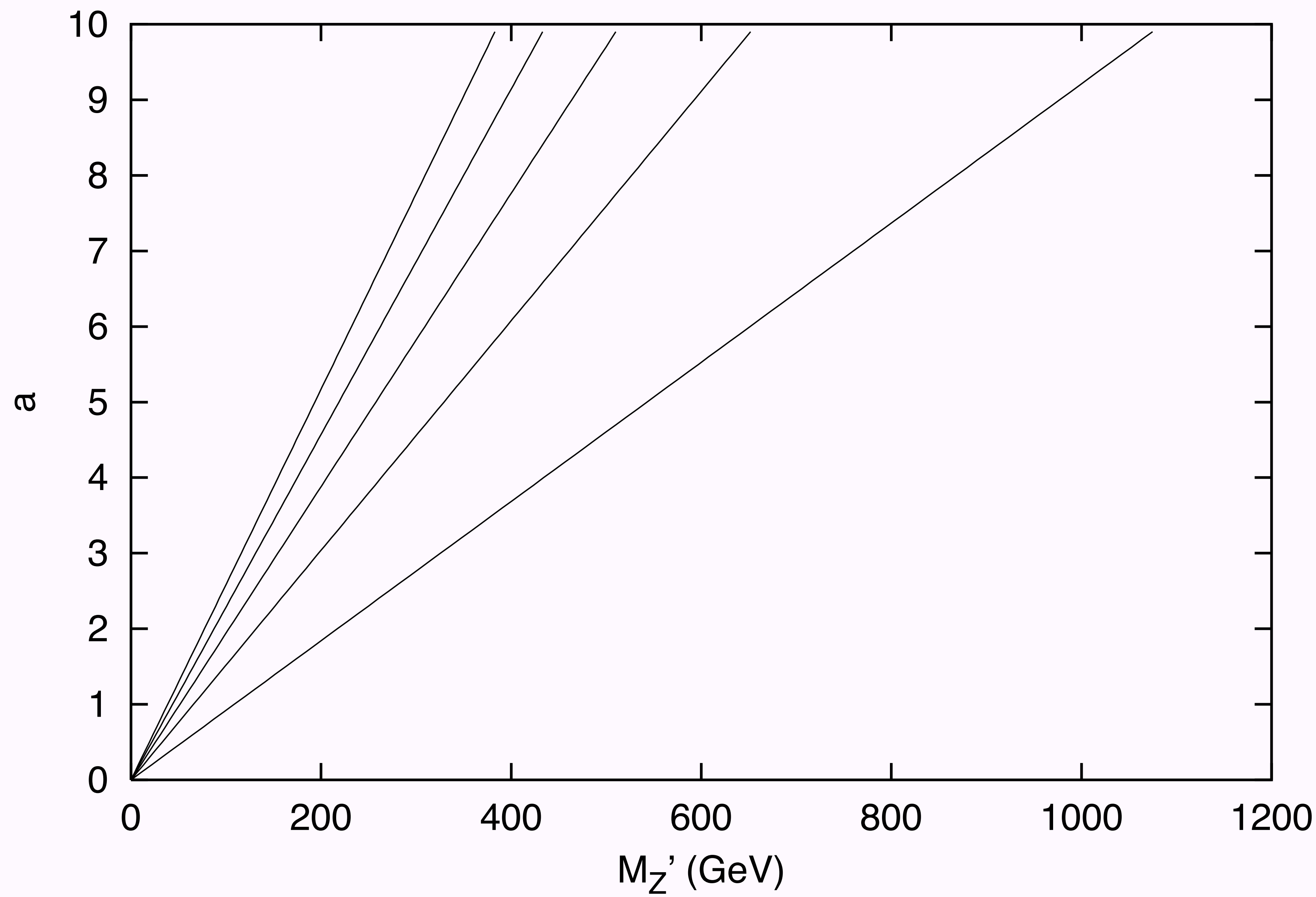

FIG. 2. Δa_μ on the a vs. $m_{Z'}$ plane in case b). The lines from left to right are for Δa_μ away from its central value at $+2\sigma, +1\sigma, 0, -1\sigma$ and -2σ, respectively.

Collider Signatures

$$Z^{'} \to \mu^+\mu^-, \tau^+\tau^-, \nu_\alpha\bar{\nu}_\alpha \text{ (with } \alpha = \mu \text{ or } \tau\text{)},\ \psi_D\overline{\psi}_D\ ,$$

$$\Gamma(Z^{'} \to \mu^+\mu^-) = \Gamma(Z^{'} \to \tau^+\tau^-) = 2\Gamma(Z^{'} \to \nu_\mu\bar{\nu}_\mu) = 2\Gamma(Z^{'} \to \nu_\tau\bar{\nu}_\tau) = \Gamma(Z^{'} \to \psi_D\bar{\psi}_D)$$

$$\Gamma_{\rm tot}(Z^{'}) = \frac{\alpha^{'}}{3}\, M_{Z'} \times 4(3) \approx \frac{4(\text{or } 3)}{3}\ \text{GeV} \left(\frac{\alpha^{'}}{10^{-2}}\right) \left(\frac{M_{Z'}}{100\text{GeV}}\right)$$

The dominant mechanisms of $Z^{'}$ productions at available colliders are

$$\begin{aligned} q\bar{q}\ (\text{or } e^+e^-) &\to \gamma^*, Z^* \to \mu^+\mu^- Z^{'}, \tau^+\tau^- Z^{'} \\ &\to Z^* \to \nu_\mu\bar{\nu}_\mu Z^{'}, \nu_\tau\nu_\tau Z^{'} \end{aligned}$$

There are also vector boson fusion processes such as

$$\begin{aligned} W^+W^- &\to \nu_\mu\bar{\nu}_\mu Z^{'}\ \ (\text{or } \mu^+\mu^-\text{Z}^{'}), \quad \text{etc.} \\ Z^0Z^0 &\to \nu_\mu\bar{\nu}_\mu Z^{'}\ \ (\text{or } \mu^+\mu^-\text{Z}^{'}), \quad \text{etc.} \\ W^+Z^0 &\to \nu_\mu\bar{\mu} Z^{'}\ \ (\text{or } \mu^+\mu^-\text{Z}^{'}), \quad \text{etc.} \end{aligned}$$

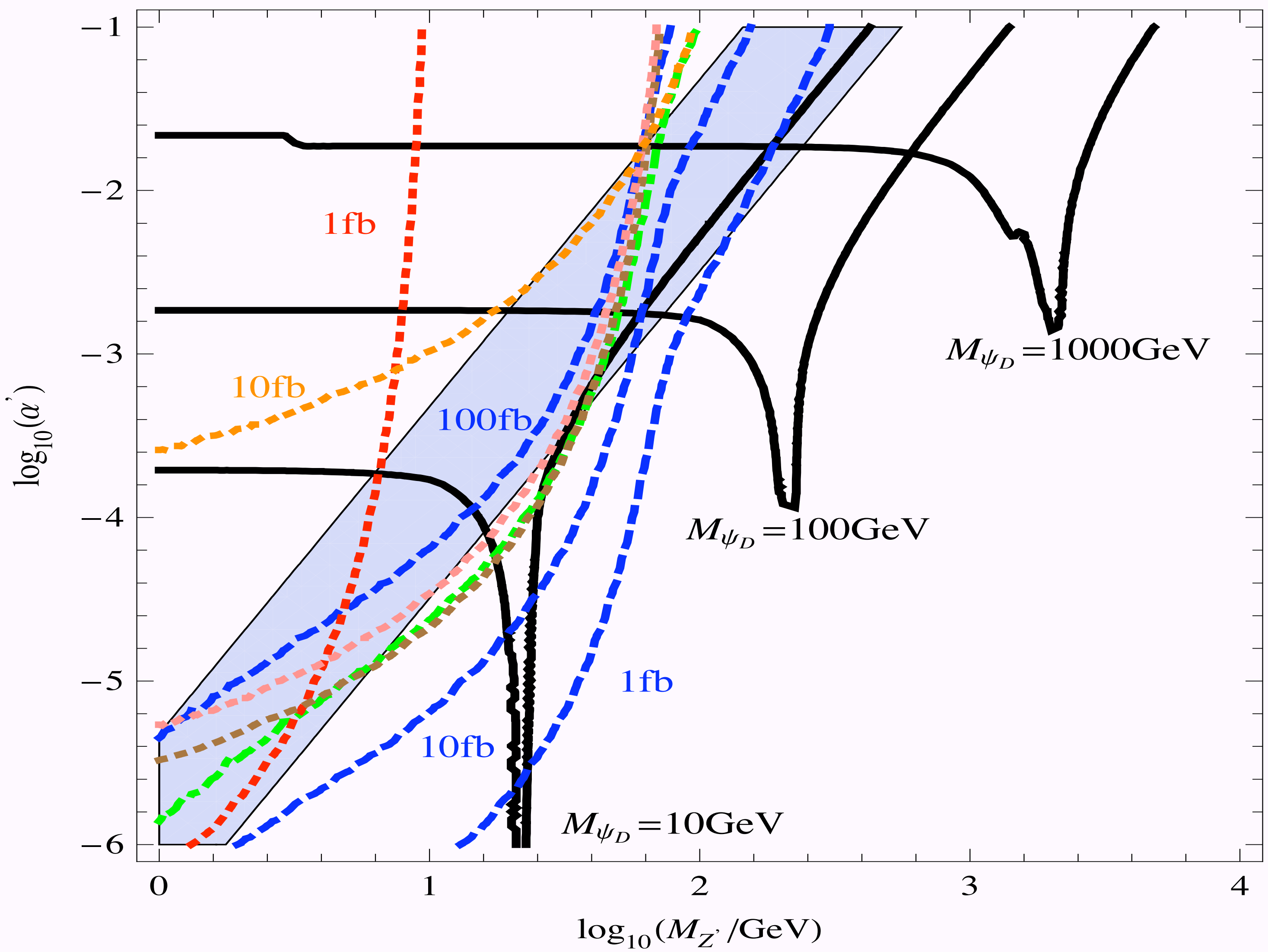

Figure 1: The relic density of CDM (black), the muon $(g-2)_\mu$ (blue band), the production cross section at B factories (1 fb, red dotted), Tevatron (10 fb, green dotdashed), LEP (10 fb, pink dotted), LEP2 (10 fb, orange dotted), LHC (1 fb, 10 fb, 100 fb, blue dashed) and the Z^0 decay width (2.5×10^{-6} GeV, brown dotted) in the $(\log_{10}\alpha', \log_{10} M_{Z'})$ plane. For the relic density, we show three contours with $\Omega h^2 = 0.106$ for $M_{\psi_D} = 10$ GeV, 100 GeV and 1000 GeV. The blue band is allowed by $\Delta a_\mu = (302 \pm 88) \times 10^{-11}$ within 3 σ.

Higgs Searches

- The mixing term $\lambda_{H\phi}$ can make the Higgs search non-standard.

$$\begin{aligned} h_{\rm SM} &= H_1 \cos\alpha - H_2 \sin\alpha, \\ s &= H_1 \sin\alpha + H_2 \cos\alpha, \end{aligned}$$

- $\tan\beta = v_\phi / v_{\rm SM}$.

Figure 2: In the left (right) column are shown the branching ratios of the lighter (heavier) Higgs $H_{1(2)}$ into two particles in the final states: $t\bar{t}$ (solid in red), $b\bar{b}$ (dashed red), $c\bar{c}$ (dotted red), $s\bar{s}$ (dot-dashed red), $\tau\bar{\tau}$ (solid orange), $\mu\bar{\mu}$ (dashed orange), WW (dashed blue), ZZ (dotted blue) and $Z^{'}Z^{'}$ (solid blue) for difference values of the mixing angle α and $\tan\beta$. We fixed $M_{Z'} = 300$ GeV. We also fixed $M_{H_2} = 700$ GeV ($M_{H_1} = 150$ GeV) for the plots of the left (right) column.

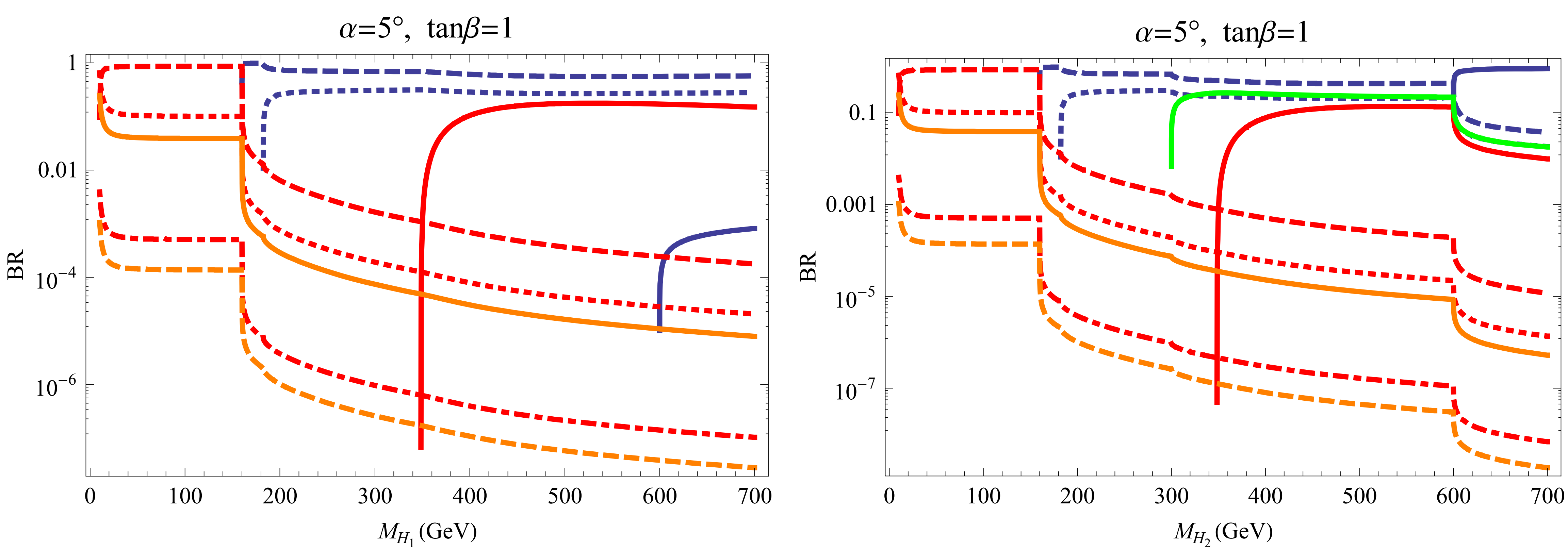

Higgs Searches

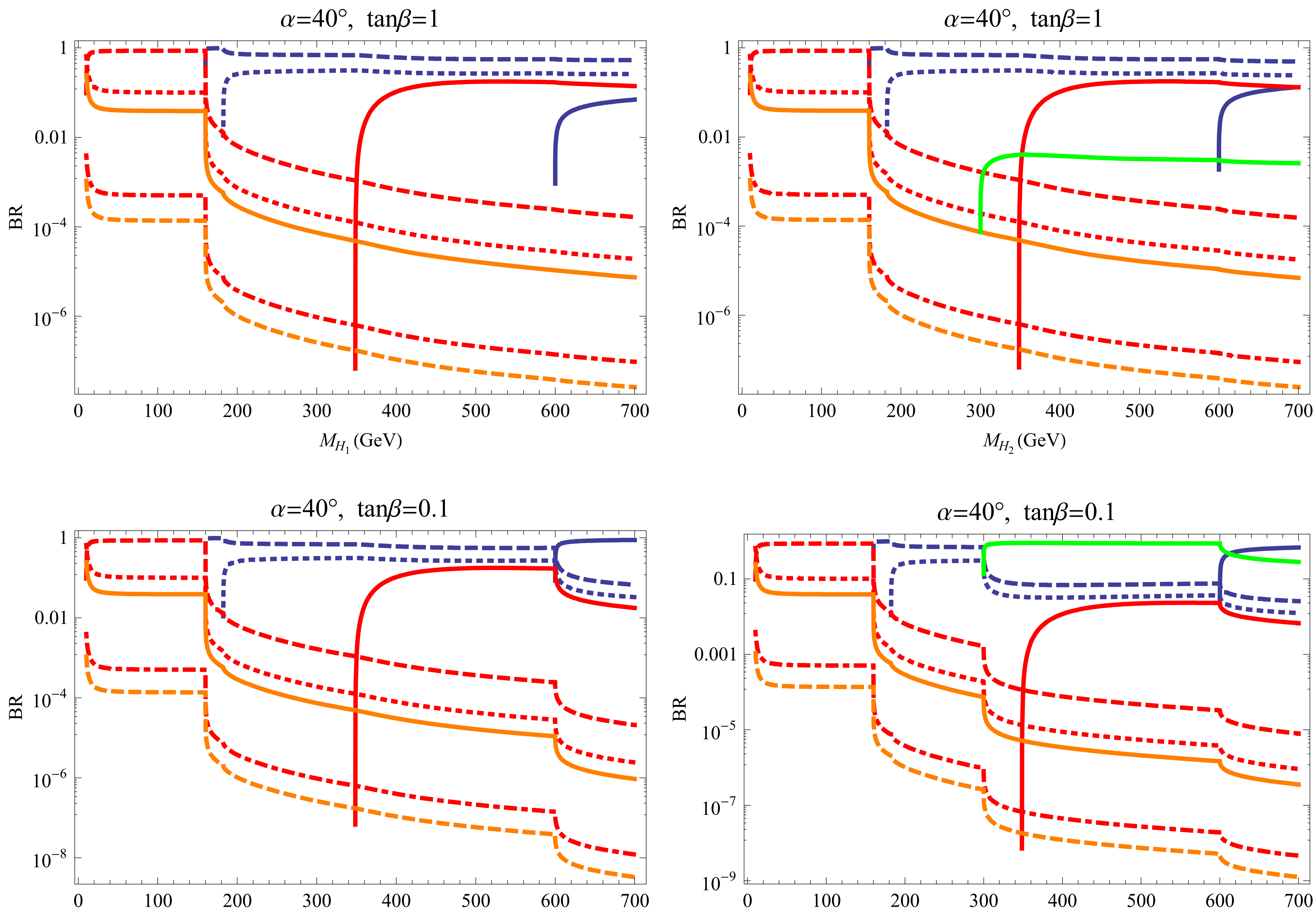

Sommerfeld enhancement

- If DM is a thermal relic, the relic abundance is approximately given by

$$\Omega h^2 \simeq 0.1 \times \left(\frac{3 \times 10^{-26}\mathrm{cm}^3/\mathrm{sec}}{\langle \sigma v \rangle_{\mathrm{freeze}}} \right). \qquad (1)$$

- The PAMELA, ATIC suggest $\sigma v \approx 10^{-23}\mathrm{cm}^3/\mathrm{sec}$

Sommerfeld enhancement

The large "boost factor" can come from

- the clumpy distribution of the dark matter
- or the "Sommerfeld enhancement". (A. Sommerfeld (1931)) For long range force and small $v(\sim 10^{-3})$, a bound state can be formed before annihilation (Arkani-Hamed *et.al*, arXiv:0810.0713)

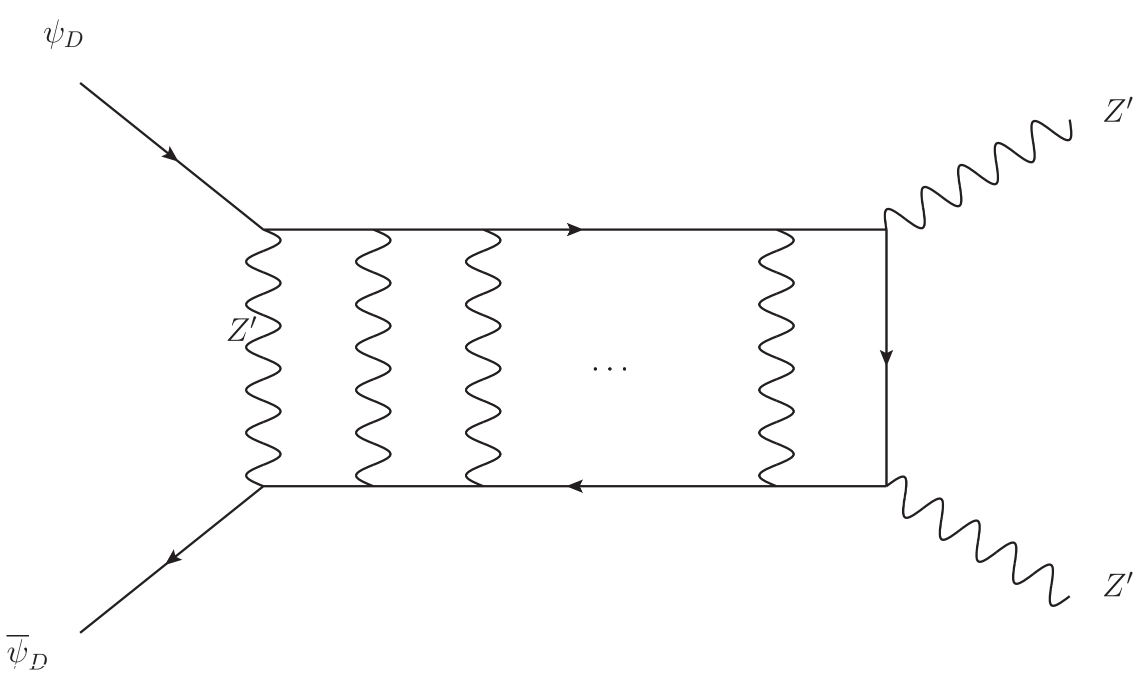

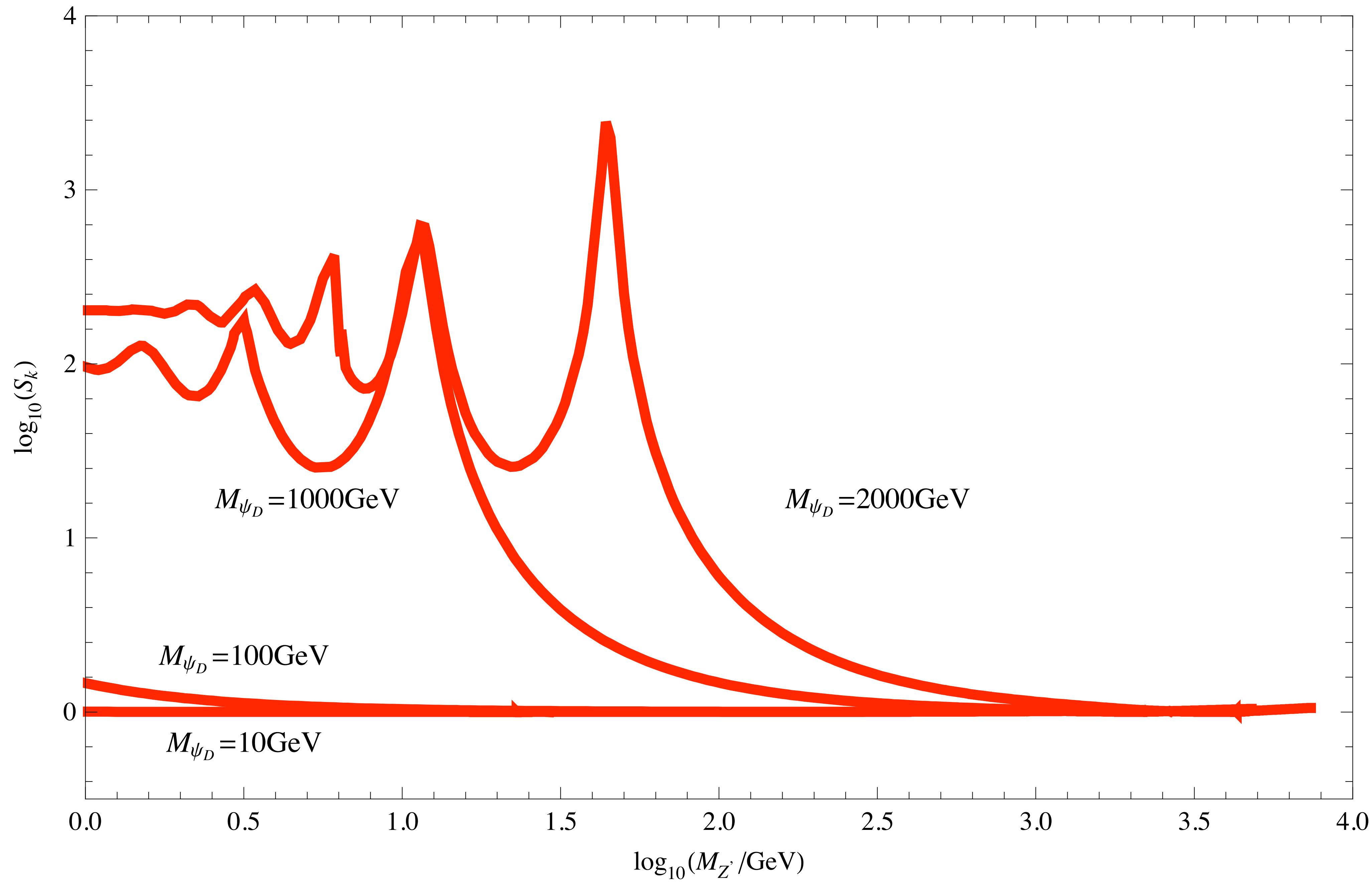

Figure: Sommerfeld enhancement factor along the constant relic density lines. $v = 200$ km/s.

PAMELA, Fermi LAT, HESS, SK, HESS gamma-ray from GC

- Fit the BF, and scale parameters to the indirect detection data
- Used NFW DM profile with MED parameters
- For the background e^- and e^- we used the results in Baltz and Edsjö (1998); Moskalenko and Strong (1998)
- Considered SK up-going neutrino-induced muon flux, HESS gamma-ray frux from the GC

$L_\mu - L$

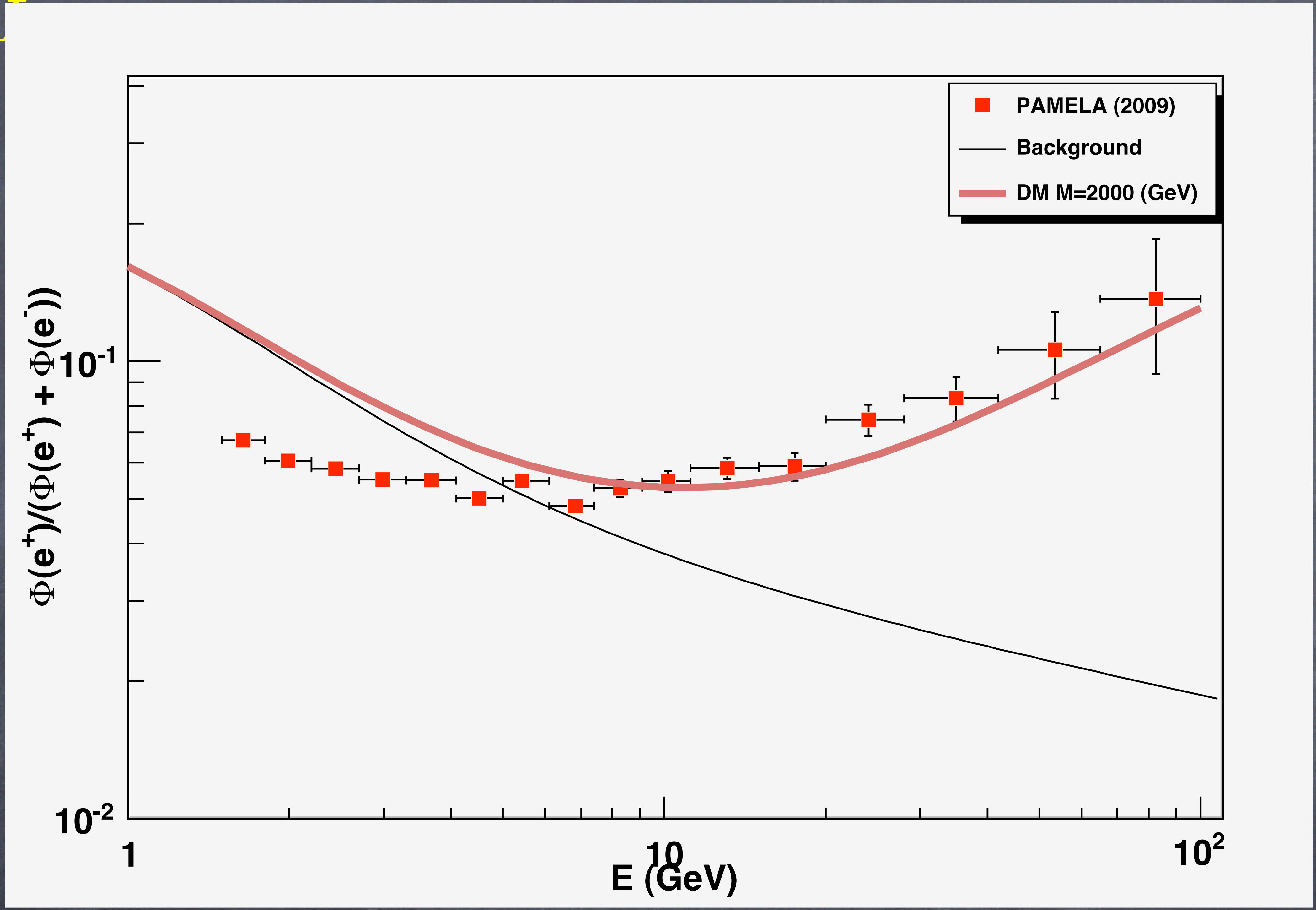

PAMELA positron ratio to (electro + positron)

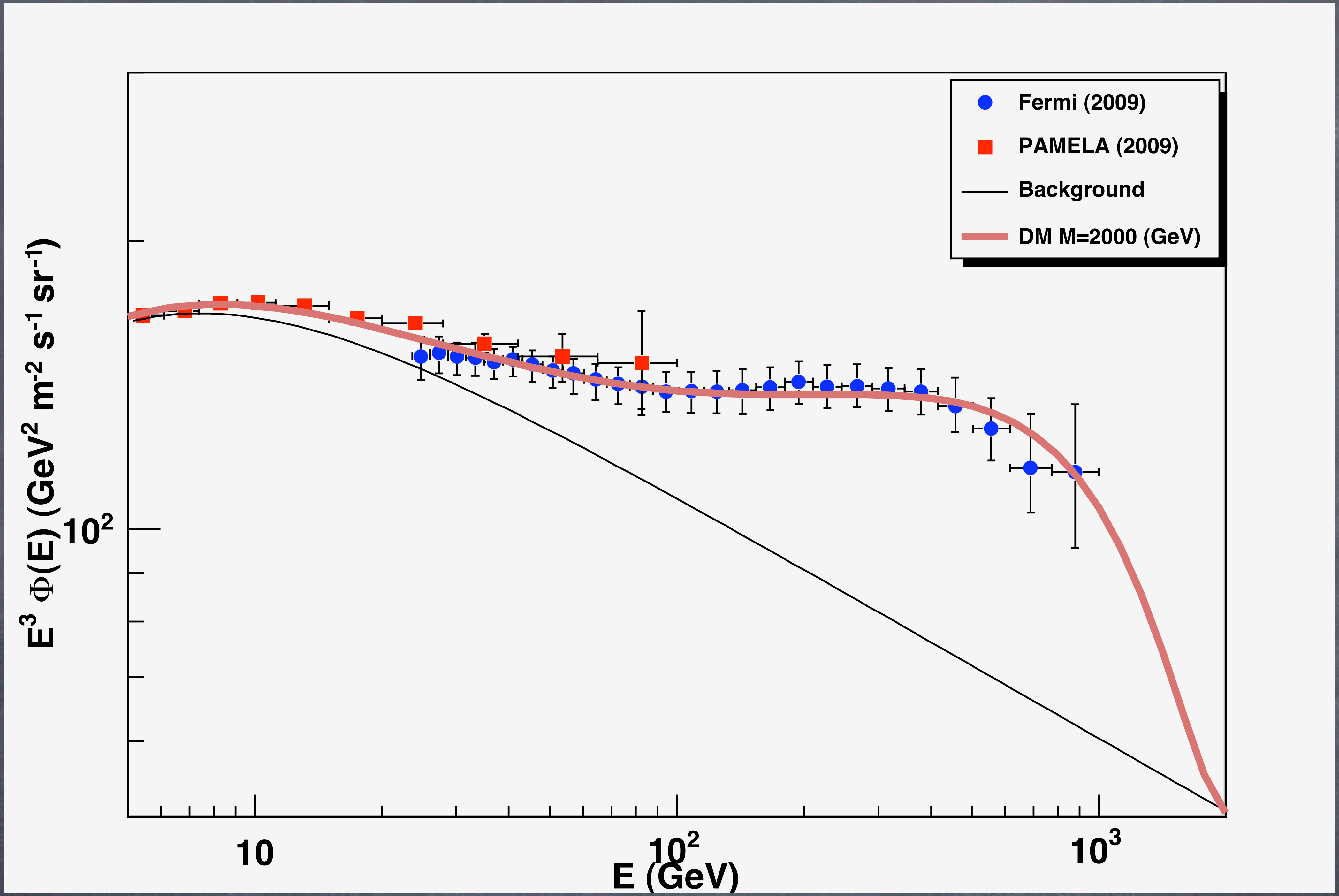

PAMELA + FERMI with bkgd x 0.67 and large boost factor ~O(5000)

Fit to PAMELA data

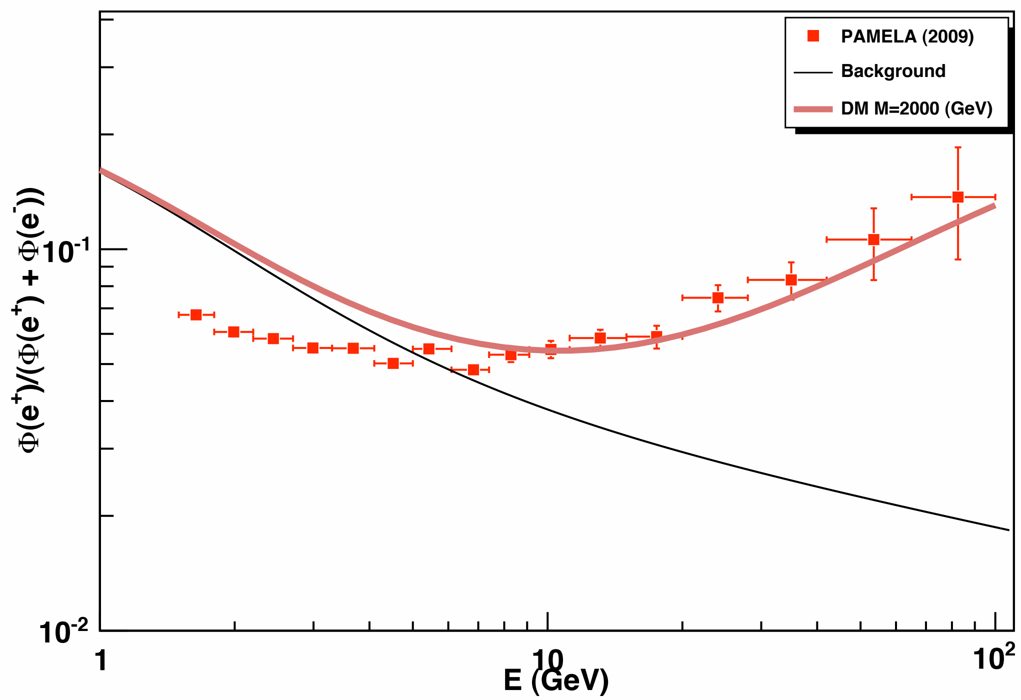

Fit to PAMELA, Fermi LAT, and HESS data

NFW MED, BF=1574, $\chi^2_{\min}/dof = 201/50$.

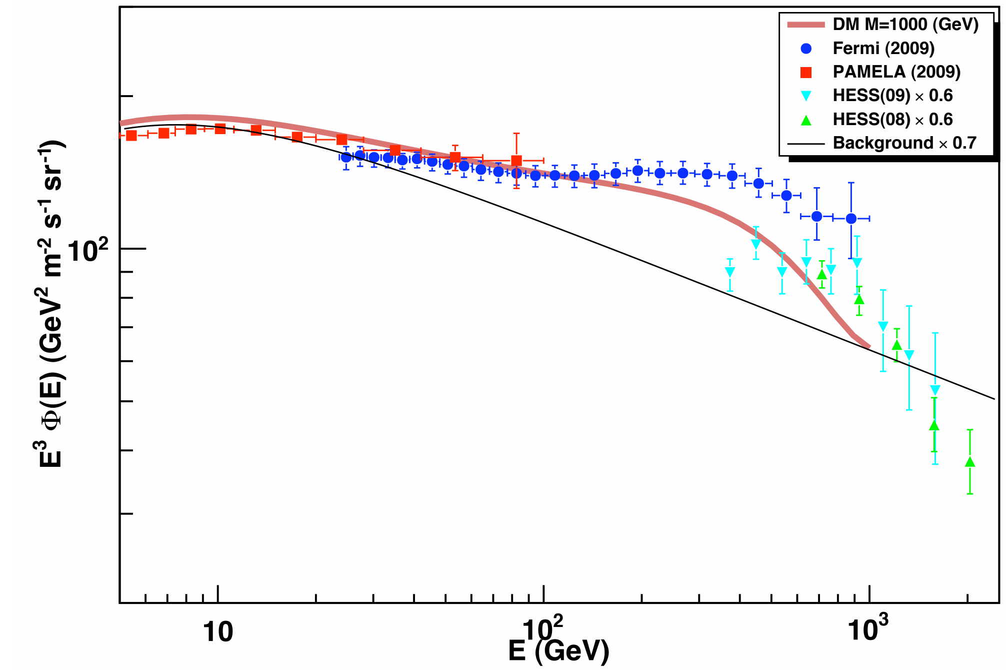

Fit to PAMELA, Fermi LAT, and HESS data

NFW MED, BF=3044, $\chi^2_{\min}/dof = 104/50$.

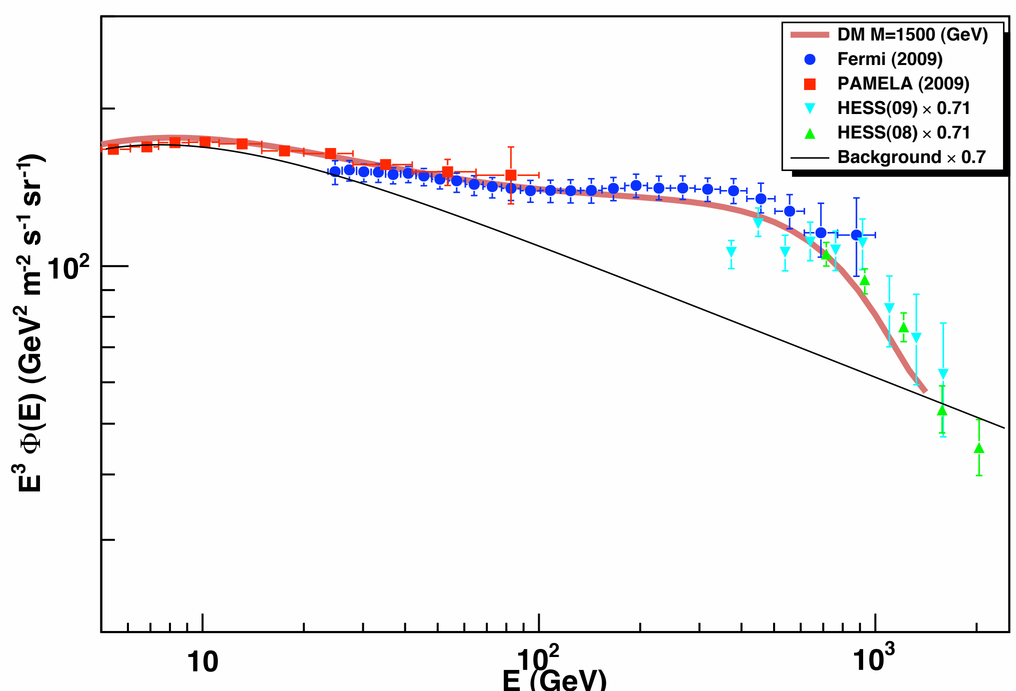

Fit to PAMELA, Fermi LAT, and HESS data

NFW MED, BF=5198, $\chi^2_{\min}/dof = 53/50$.

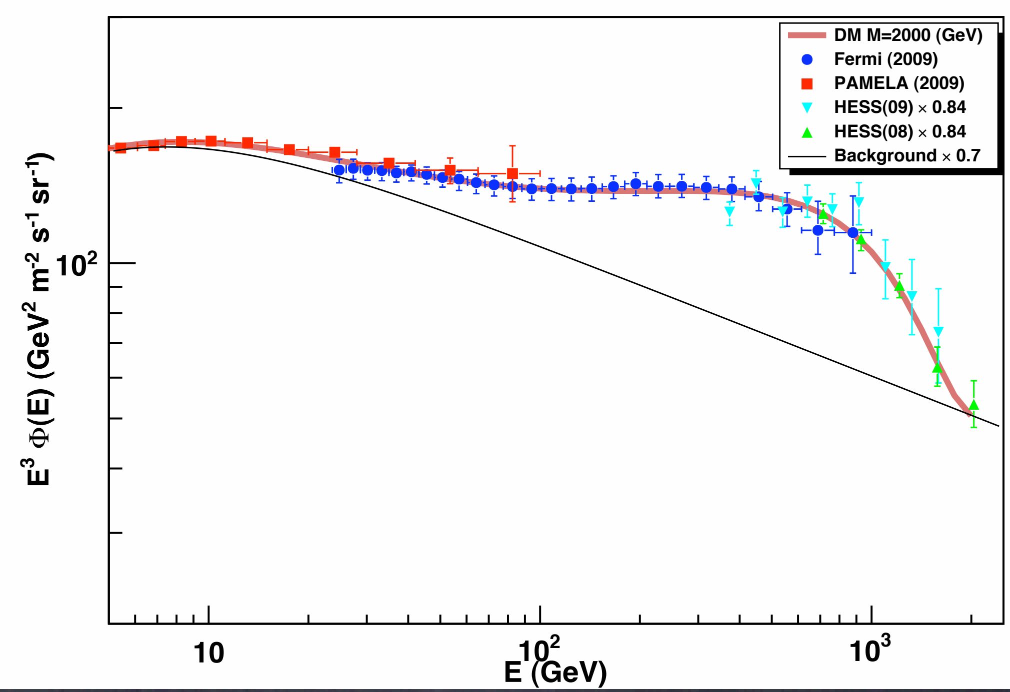

DM density profiles

$$\rho(r, r_s) = \frac{1}{r^\gamma} \frac{\rho_0}{(1 + (r/r_s)^\alpha)^{(\beta-\gamma)/\alpha}}$$

Halo model	α	β	γ	r_s [kpc]
Cored isothermal	2	2	0	5
Navarro, Frenk & White	1	3	1	20
Moore	1.5	3	1.3	30

Table: Dark matter distribution profiles in the Milky Way.

DM density profiles

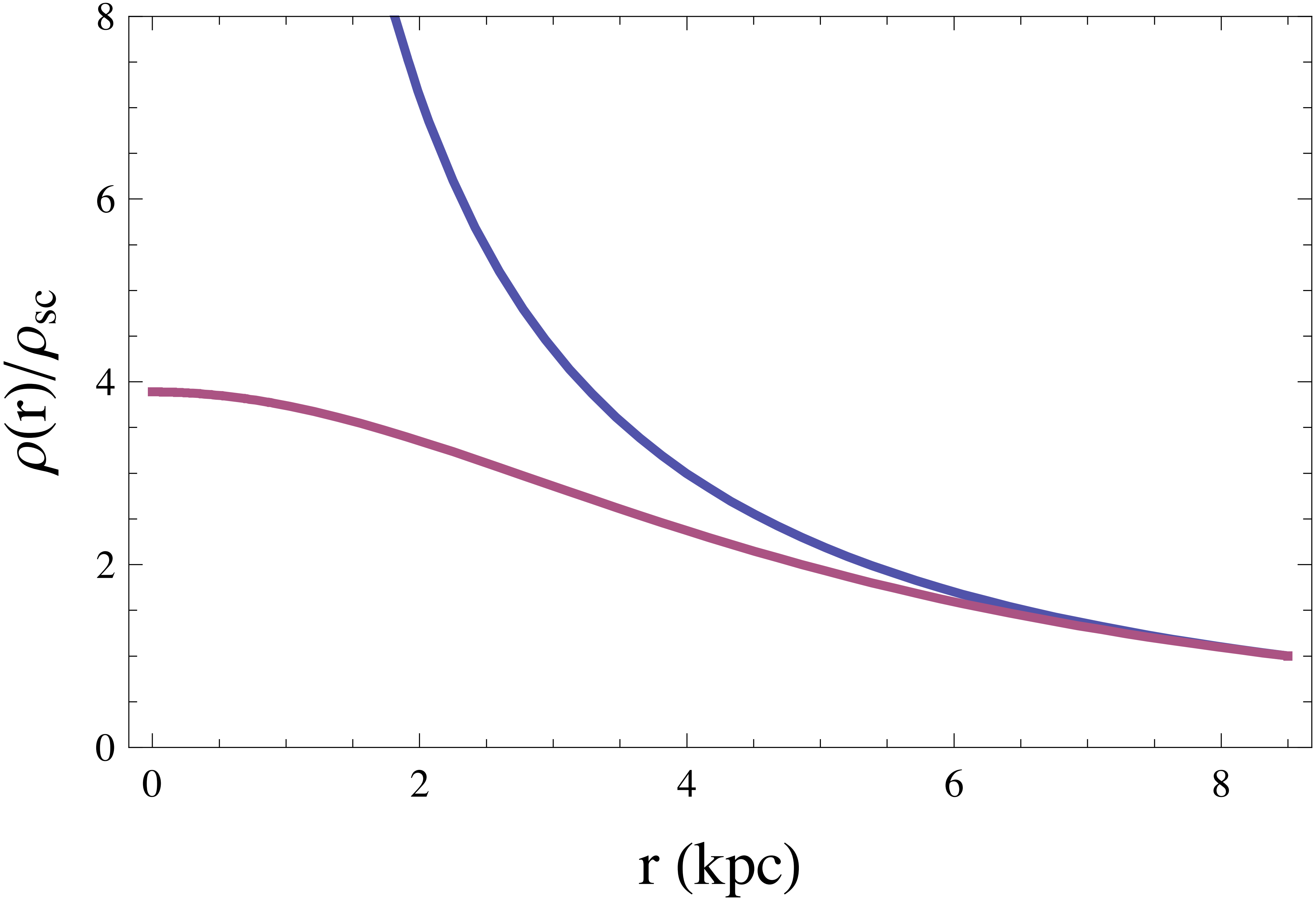

SK Constraint on upgoing muon flux

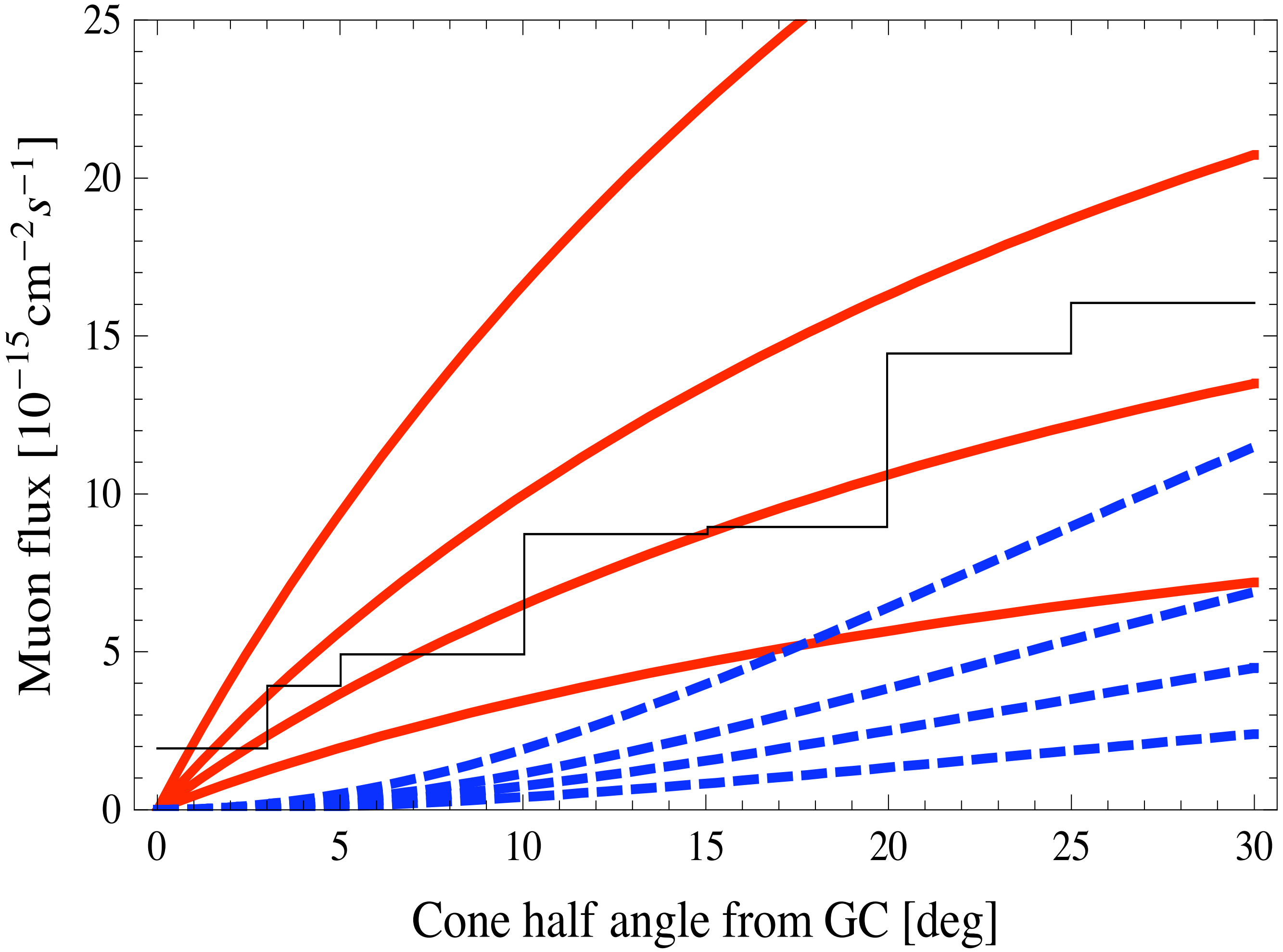

Figure 5: Thick solid red curves (thick dashed blue curves) are predictions of the neutrino-induced up-going muon flux from the annihilation of dark matter with masses 3, 2, 1.5, 1 TeV from above, for the NFW (isothermal) dark matter profile. The thin solid line is the superkamiokande bound.

Gamma ray flux constraint (HESS)

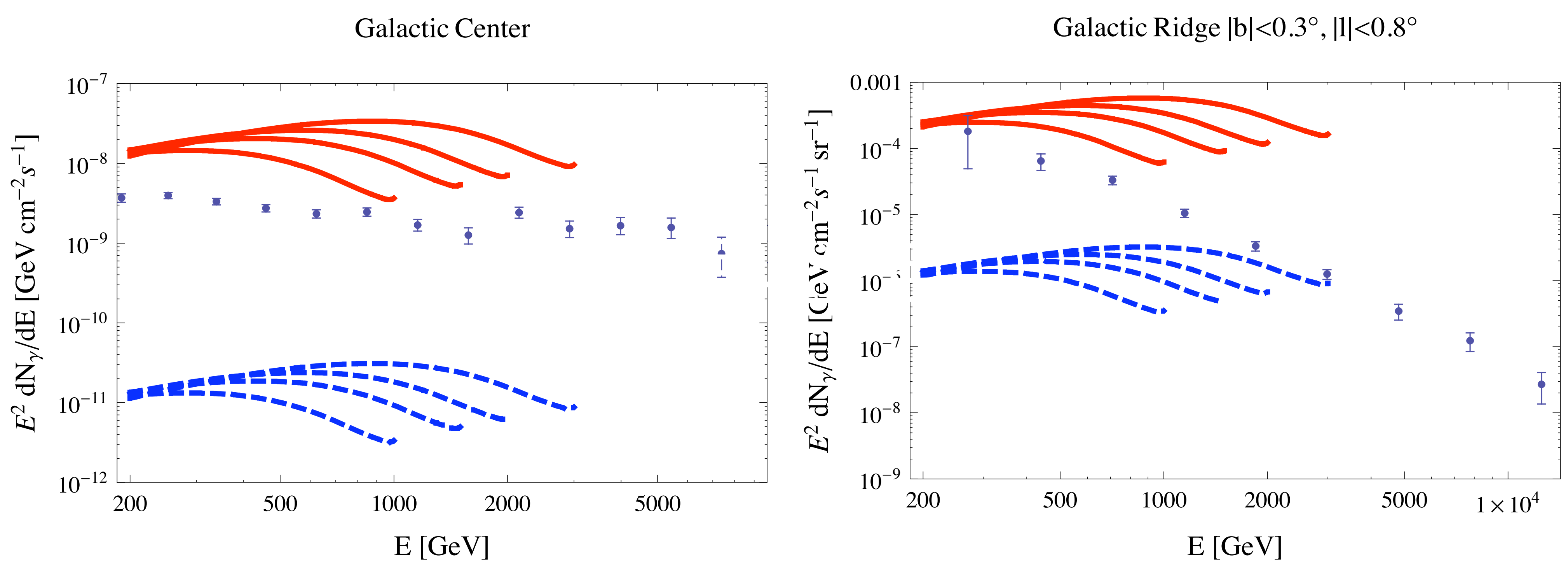

Figure 6: The gamma ray flux from the GC (left panel) and GC ridge (right panel). Thick solid red curves (thick dashed blue curves) are predictions of the gamma ray flux from the annihilation of dark matter with masses 3, 2, 1.5, 1 TeV from above, for the NFW (isothermal) dark matter profile.

Conclusions

- DM from leptophilic $U(1)_{L_\mu - L_\tau}$ model can be an explanation of positron/electron excess in PAMELA, Fermi LAT and HESS CR experiments.
  - the fit to the data is excellent when $M_{\rm DM} = 2000$ GeV
  - the required BF can be obtained from the Sommerfeld enhancement
  - $M_{\rm DM} = 2000$ GeV is only marginally allowed. $M_{\rm DM} > 2000$ GeV is ruled out by SK muon flux.
  - NFW density profile is disfavored by the HESS gamma-ray data. The isothermal profile is consistent with the data.
- LHC can cover the large parameter space of $U(1)_{L_\mu - L_\tau}$ model through multi muon/tau events.
- The Higgs searches can be non-standard.

For other approaches for leptophobic/leptophilic CDM

- Ko and Yuji Omura, SUSY U(1)B x U(1)L, arXiv: 1012.4679, to appear in PLB
- Ko, Omura and Yu, Dijet resonance from leptophobic Z' and light baryonic DM, arXiv: 1104.4066
- Gondolo, Ko, Omura, Light DM in leptophobic Z' model, arXiv: 1106.0885
- Indirect signatures in these models under study